Journal of Organometallic Chemistry, 449 (1993) 9–18

JOM 23375

Low-temperature organometallic synthesis of crystalline and glassy ternary semiconductors $M^{II}M^{IV}P_2$ where M^{II} = Zn and Cd, and M^{IV} = Ge and Sn

Subhash C. Goel and William E. Buhro

Department of Chemistry, Washington University, St. Louis, MO 63130 (USA)

Natalie L. Adolphi and Mark S. Conradi

Physics Department, Washington University, St. Louis, MO 63130 (USA)

(Received August 3, 1992)

Abstract

The first organometallic syntheses of the ternary phosphides $M^{II}M^{IV}P_2$ (M^{II} = Zn, Cd; M^{IV} = Ge, Sn) are described. Reactions between the precursors $\{M^{II}[P(SiMe_3)_2]_2\}_2$ and $M^{IV}X_4$ (X = OMe, Cl) afford the intermediates $[M^{II}M^{IV}P_2(X)_x(SiMe_3)_x]$ with $x = 0.3–0.8$, which are converted to amorphous $M^{II}M^{IV}P_2$ compounds by annealing at 250–350°C *in vacuo*. The amorphous compounds crystallize to the corresponding chalcopyrite phases at low temperatures, providing the lowest synthesis temperatures yet reported by any synthetic method: $ZnGeP_2$, 700–800°C; $CdGeP_2$, 500–650°C; $ZnSnP_2$, 350–600°C; $CdSnP_2$, 250–450°C. The solid-state MAS ^{31}P NMR spectrum of the amorphous $CdGeP_2$ contains a single feature centered at −104 ppm relative to H_3PO_4 (full width at half maximum, 160 ppm). Spin-echo experiments on a nonspinning sample determine that $T_2 = 350$ μs. These data are indistinguishable from data for glassy $CdGeP_2$ obtained from conventional melt quenching, suggesting that the amorphous $CdGeP_2$ phases prepared by the two techniques have very similar or identical structures. Analogies between the new organometallic syntheses and the sol-gel process for oxides are discussed.

1. Introduction

Herein we report organometallic routes to the II–IV–V_2 semiconductors $ZnGeP_2$, $CdGeP_2$, $ZnSnP_2$, and $CdSnP_2$. To our knowledge these are the first organometallic syntheses of a family of ternary materials. The II–IV–V_2 compounds have potential applications in light-emitting diodes, in infrared detectors and generators, in IR-transmitting ceramics, as nonlinear optical materials, and as variable-band-gap semiconductors [1–4]. The II–IV–V_2 compounds are conventionally prepared by high-temperature techniques, including crystallization from the melt, crystallization from a metal flux (such as Sn or Zn), and chemical vapor transport [1,5].

Recently, new strategies for the synthesis of binary semiconductors have emerged that are based on organometallic elimination reactions [6–14]. The antecedent to the current efforts was most likely the development of MOCVD using metal alkyls and nonmetal hydrides [14]. The new organometallic techniques have been undertaken to address a variety of goals, and we particularly emphasize the following. Organometallic syntheses generally proceed at considerably lower temperatures than conventional methods [6–14]. Thus, they may facilitate the intergration of the semiconductors into devices having heat-sensitive components, and avoid impurities arising from side reactions with container materials in high-temperature procedures. Organometallic syntheses allow the preparation of size- and morphology-controlled nanoclusters [6,11,15–18]. By analogy to the sol-gel process [19], organometallic syntheses might also afford viscous sols and gels that could be processed to give fibers, films, powders, and monoliths. Organometallic syntheses should provide

Correspondence to: Professor W.E. Buhro.

0022-328X/93/$6.00

kinetic routes to semiconductor materials in new forms and phases that are inaccessible from high temperatures. We now report significant reductions in the synthesis temperatures for crystalline II–IV–V_2 chalcopyrite phases over conventional techniques, and observations bearing on the ability of our organometallic syntheses to address the outlined purity and processing goals. A portion of the work has already been published [12].

Some II–IV–V_2 compounds may be obtained as glasses by quenching from the melt [20]; among these, $CdGeP_2$ has been particularly well studied recently [21]. The present study has provided a rare opportunity to compare such a glassy semiconductor obtained conventionally (by melt quenching) with an analogous amorphous semiconductor prepared at low temperature. Syntheses based on organometallic elimination reactions typically yield amorphous products initially, which may be annealed to give crystalline phases under mild conditions [6–14]. The question arises, how do these initially obtained amorphous materials compare with conventional glasses? We have compared our amorphous $CdGeP_2$ prepared at low temperature with glassy $CdGeP_2$ obtained from the melt. On the basis of physical and spectroscopic properties, we find them to be very similar. The results suggest that the $CdGeP_2$ glasses made from "the top down" (melt quenching) and from "the bottom up" (organometallic synthesis) have structures that are closely related, and indeed they are probably isostructural. Oxide glasses prepared by low-temperature organometallic sol-gel routes and the corresponding oxide glasses prepared by quenching from high-temperature melts are generally found to be isostructural [22]. However, to our knowledge structural comparisons of conventional and organometallic-precursor-derived nonoxide glasses are not available.

2. Results and discussion

2.1. Synthesis and characterization

The chalcopyrite structure of the II–IV–V_2 compounds, including the $M^{II}M^{IV}P_2$ compounds of interest here, is related to the cubic, zinc-blende structure [23]. All atoms are tetrahedrally coordinated; M^{II} and M^{IV} atoms have four covalently bonded P nearest neighbors, and P atoms have two M^{II} and two M^{IV} covalently bonded nearest neighbors. Consequently, organometallic syntheses must be devised to construct the covalent M–P bonds and to incorporate the three elements in the appropriate ratios. Several of the organometallic syntheses of binary semiconductors (ME) use the general elimination strategy shown in eqn. (1) [7,9–11,13], in which the bimolecular elimination of Me_3Si–X (X = halide, alkyl, acetylacetonate) drives the formation of M–E covalent bonds. We adapted this general strategy to the synthesis of the ternary $M^{II}M^{IV}P_2$ semiconductors as described below.

$$M - X + E - SiMe_3 \longrightarrow M - E + X - SiMe_3 \quad (1)$$

Our organometallic precursors were the disilylphosphido complexes $\{Zn[P(SiMe_3)_2]_2\}_2$ and $\{Cd[P(SiMe_3)_2]_2\}_2$, which have the structure **I** shown below [12,24]. Note that the ratio of M^{II}/P in the precursors is 1:2 as required, and that the $P(SiMe_3)_2$ ligands have the correct number of $SiMe_3$ groups to incorporate M^{IV} with the required stoichiometry by eqn. (1) eliminations. Consequently, we examined the elimination reactions between the precursors $\{M^{II}[P(SiMe_3)_2]_2\}_2$ (M^{II} = Zn, Cd) and $M^{IV}(OMe)_4$ or $M^{IV}Cl_4$ (M^{IV} = Ge, Sn), and found that they proceeded according to eqns. (2) or (3), respectively.

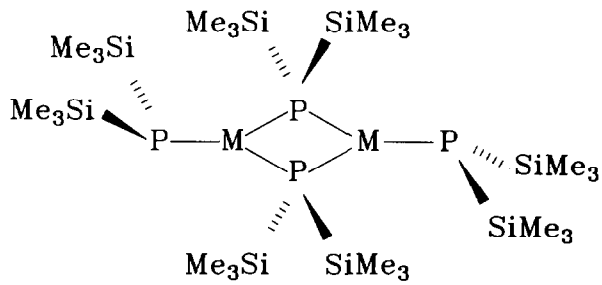

Equations (2) and (3) were completed in a series of stages. In all cases the elimination reactions ensued

$$1/2\{M^{II}[P(SiMe_3)_2]_2\}_2 + M^{IV}(OMe)_4 \xrightarrow[\text{toluene}]{-(4-x)MeOSiMe_3} [M^{II}M^{IV}P_2(OMe)_x(SiMe_3)_x] \xrightarrow[\text{solid state}]{\Delta} M^{II}M^{IV}P_2 + x\,MeOSiMe_3$$

M^{II} = Zn	M^{IV} = Ge	$x = 0.5$
Cd	Ge	0.3
Zn	Sn	0.5
Cd	Sn	0.4

(2)

$$1/2\{M^{II}[P(SiMe_3)_2]_2\}_2 + M^{IV}Cl_4 \xrightarrow[\text{toluene}]{-(4-x)ClSiMe_3} [M^{II}M^{IV}P_2(Cl)_x(SiMe_3)_x] \xrightarrow[\text{solid state}]{\Delta} M^{II}M^{IV}P_2 + xClSiMe_3$$

M^{II} = Zn	M^{IV} = Ge	$x = 0.6$
Cd	Ge	0.8
Zn	Sn	0.8
Cd	Sn	0.5

(3)

upon combination of the precursors in room-temperature toluene solutions; the Me_3SiX (X = OMe, Cl) compounds were the only byproducts detected by ^1H

NMR monitoring. Some of the solutions darkened but remained homogeneous; others formed precipitates, sols, or gels as elaborated below. Then the mixtures were refluxed for several hours whereupon dark precipitates were obtained in all cases. The elemental analyses of the insoluble, air-sensitive precipitates fit the empirical formulae $[M^{II}M^{IV}P_2\text{-}(X)_x(SiMe_3)_x]$ where X = OMe or Cl and x varied from 0.3 to 0.8 (see eqns. (2) and (3)). Infrared spectra confirmed the residual OMe and $SiMe_3$ groups. Therefore, the solution-phase conditions employed were not sufficient to complete the thermal elimination of Me_3SiX.

The $[M^{II}M^{IV}P_2(X)_x(SiMe_3)_x]$ intermediates were next heated in the solid state to 250–350°C under dynamic vacuum (10^{-2} Torr). This step completed the removal of Me_3SiX. In several of the experiments, the volatile organic byproducts were collected and analyzed. They were found to be exclusively the expected Me_3SiX compounds; no other byproducts such as $Me_3SiSiMe_3$, MeO_2Me, Me_2O, or Cl_2 were detected. Thus, we conclude that eqns. (2) and (3) proceeded cleanly to form new M–P bonds and not P–P or M–M bonds; this will be important below. The resulting solids were amorphous $M^{II}M^{IV}P_2$ compounds except that $ZnSnP_2$ and $CdSnP_2$ were just beginning to crystallize at temperatures of 350 and 250°C, respectively. All were at least moderately air stable.

TABLE 1. Melting points and synthesis temperatures of crystalline $M^{II}M^{IV}P_2$ compounds

Compound	m.p. (°C)	Lowest conventional synthesis temp. (°C)	Organometallic synthesis temp. (°C)
$ZnGeP_2$	1025, [a] congruent	950–980 [b]	700–800 [c]
$CdGeP_2$	776–800, [a,d] congruent	800 [e]	500–650 [c]
$ZnSnP_2$	930, [a] incongruent	800 [f]	350–600 [c]
$CdSnP_2$	570, [a] incongruent	520–570 [g,h]	250–450 [c]

[a] Ref. 1, p. 11. [b] Ref. 5. [c] This work; the low temperature corresponds to the emergence of a resolved XRD pattern, the high temperature is the limit for further resolution improvements. [d] The T_g for glassy $CdGeP_2$ obtained by quenching from the melt is 445–450°C [21] and the crystallization temperature is 500°C [29]. [e] Ref. 21. [f] Ref. 36. [g] Ref. 37. [h] Ref. 38.

The crystallization of the amorphous $M^{II}M^{IV}P_2$ compounds was studied by annealing the samples for several hours at progressively higher temperatures and monitoring by X-ray powder diffraction (XRD). Crystallization occurred over *ca.* 200°C ranges, and at the temperatures recorded in Table 1. Clearly resolved reflections corresponding to the chalcopyrite phases had emerged at the low end of the ranges; these

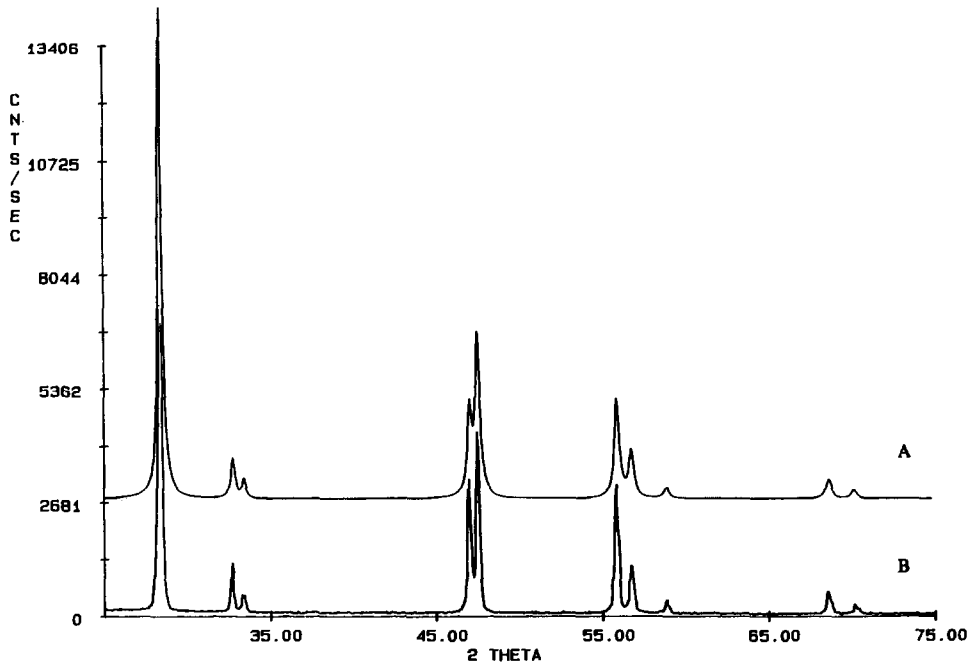

Fig. 1. Simulated (A) and observed (B) XRD patterns for organometallic-derived crystalline $ZnGeP_2$.

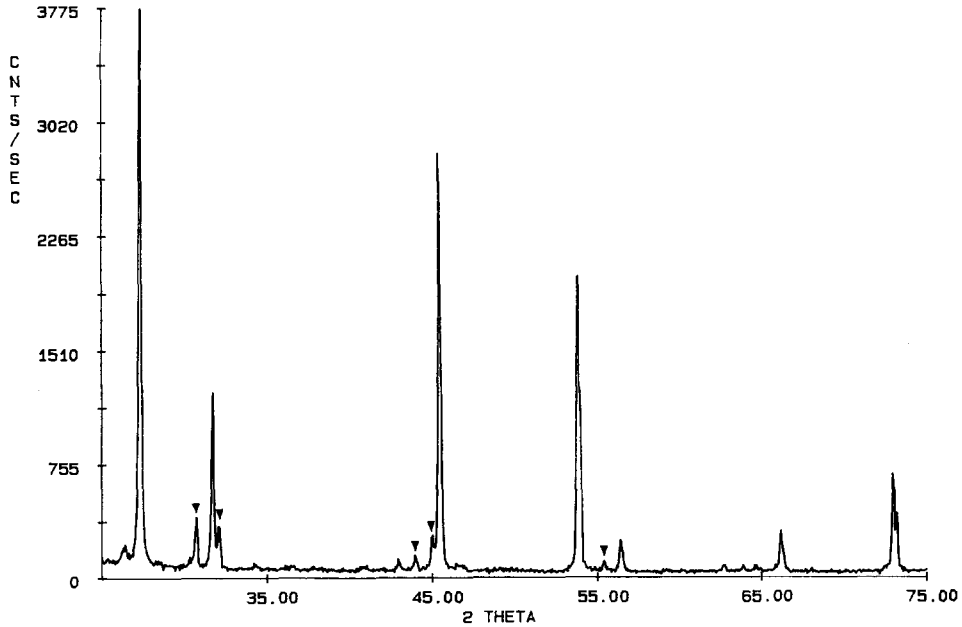

Fig. 2. XRD pattern for organometallic-derived crystalline $ZnSnP_2$; reflections due to a β-Sn impurity are labeled (▼).

reflections continued to sharpen over the stated ranges as the crystalline domains grew. The observed crystallization temperatures were 200–400°C lower than have been obtained by conventional methods (see Table 1), and to our knowledge they represent the lowest reported temperatures for the synthesis of crystalline $M^{II}M^{IV}P_2$ chalcopyrites. We believe that the low crystallization temperatures reflect the efficient atomic-scale mixing afforded by the organometallic syntheses, resulting in short diffusion distances for atoms to traverse to their equilibrium positions in the crystal lattice. Consequently, little structural reorganization was necessary to convert the amorphous $M^{II}M^{IV}P_2$ phases to crystalline phases and the activation barriers were

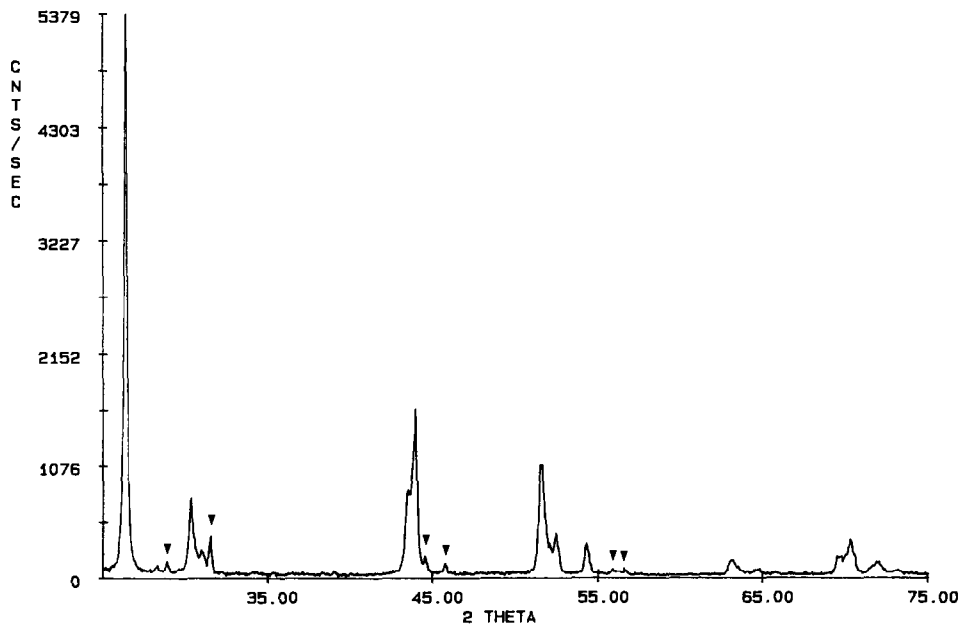

Fig. 3. XRD pattern for organometallic-derived crystalline $CdSnP_2$; reflections due to a Sn_4P_3 impurity are labeled (▼).

therefore lowered. The organometallic syntheses thus provided materials that were preorganized for crystallization. We note that organometallic, sol-gel syntheses of polymetallic oxide glasses and ceramics provide dramatically lowered processing temperatures for the same reason [19,22,25–27].

The crystalline $M^{II}M^{IV}P_2$ powders were obtained from eqns.(2) and (3) in varying degrees of chemical purity. Figure 1 shows the XRD pattern of $ZnGeP_2$ from eqn. (2), which revealed it to be phase pure. Similarly, $ZnGeP_2$ prepared by eqn. (3) and $CdGeP_2$ prepared by eqns. (2) and (3) exhibited clean, single-phase XRD patterns. Residual silicon was present in the samples in $\ll 1\%$. However, both $ZnGeP_2$ and $CdGeP_2$ contained residual carbon at levels of 1–3%, which are outside the acceptable range for electronic materials, but common for such organometallic syntheses [6–14]. We initially undertook eqn. (3) using $M^{IV}Cl_4$ reagents to determine whether less carbon incorporation would result than with eqn. (2) using $M^{IV}(OMe)_4$ reagents. Very little difference was observed. No other optimization experiments were conducted. We believe that further reaction engineering such as inclusion of annealing periods under appropriate reducing atmospheres would eliminate the carbon impurities. Interestingly, the conventional high-temperature syntheses of the $M^{II}M^{IV}P_2$ compounds are often carried out in vitreous carbon vessels [28], but because such syntheses are optimized to produce large single crystals (rather than polycrystalline powders as in our syntheses) impurities that collect at grain boundaries are incorporated only in small amounts.

Neither $ZnSnP_2$ nor $CdSnP_2$ could be obtained as phase-pure powders according to eqns. (2) and (3), but contained at least small quantities of β-Sn ($ZnSnP_2$) or Sn_4P_3 ($ZnSnP_2$, $CdSnP_2$). Representative XRD patterns are given in Figs. 2 and 3, which show the typical amounts of the impurity phases. In contrast to $ZnGeP_2$ and $CdGeP_2$, both $ZnSnP_2$ and $CdSnP_2$ melt incongruently and form peritectically. Consequently, single crystals are conventionally grown from dilute (*e.g.*, off-stoichiometric) solutions of Zn or Cd and P in molten Sn [28]; they cannot be obtained from stoichiometric mixtures. The excess Sn must be subsequently separated to purify the crystals. When the Cd–P–Sn solutions are cooled too rapidly, Sn_4P_3 precipitates as an impurity phase [28]. Obviously, $ZnSnP_2$ and $CdSnP_2$ participate in complex phase equilibria and thermal behavior. We believe that such phase equilibria occur under our Table 1 annealing conditions and produce the observed impurities. It is likely that the annealing conditions could be optimized to eliminate the impurities, as has been done for the conventional syntheses [28]. Indeed, it is significant and intriguing that $ZnSnP_2$ and $CdSnP_2$ form from the organometallic syntheses in such high purities considering that the M^{II}–Sn–P ratios are fixed at the stoichiometric values.

We have emphasized the similarity of the procedures of eqns. (2) and (3), but a few differences between them were noted. The eqn. (3) reactions using M^{IV} chlorides were more vigorous at room temperature than the analogous eqn. (2) reactions. The eqn. (2) reactions initially gave homogenous solutions at room temperature. The eqn. (3) reactions initially gave precipitates ($CdGeP_2$ and $CdSnP_2$), a viscous sol ($ZnSnP_2$), and a gel ($ZnGeP_2$) at room temperature. Recall that the sol and gel (and all other cases) were ultimately converted to crystalline chalcopyrite phases at low temperatures. The results suggest that the organometallic reactions could be optimized to generally produce sols or gels suitable for casting films or monoliths, or drawing fibers, which could then be converted to II–IV–V_2 semiconductors under mild conditions. Therefore, eqn. (3) is analogous to the popular sol-gel process for the fabrication of oxide materials [19,25–27].

2.2. Comparing conventionally derived and organometallic-derived glassy $CdGeP_2$

As described above, annealing the precipitates from eqns. (2) and (3) at 250–350°C completed the elimination of Me_3SiX and afforded amorphous $M^{II}M^{IV}P_2$ products. We sought to compare the properties of one of these products, amorphous $CdGeP_2$ prepared at 350°C, to the glassy phase obtained by quenching from the melt [20,21]. Of the four $M^{II}M^{IV}P_2$ compounds studied here, only $CdGeP_2$ can be quenched rapidly enough to afford a glass [20]. Conventionally derived $CdGeP_2$ has a T_g of 445–450°C [21], and was reported to crystallize at 500°C over several days [29]. We found that amorphous $CdGeP_2$ from the organometallic route crystallized slowly at 500°C and much more rapidly at 600°C. Therefore, conventionally and organometallic-derived amorphous $CdGeP_2$ exhibited very similar thermal behavior. Additional data were collected by solid-state ^{31}P NMR, as described below.

We compared the solid-state ^{31}P NMR data obtained from the organometallic-derived amorphous $CdGeP_2$ to the data recently reported by Eckert and co-workers in a study of conventionally derived glassy $CdGeP_2$ [21]. The solid-state MAS ^{31}P NMR spectrum of organometallic-derived amorphous $CdGeP_2$ is shown in Fig. 4. The spectrum contained a single broad feature centered at -104 ppm (relative to H_3PO_4), and having a full width at half maximum (FWHM) of 160 ppm. This is nearly identical to the spectrum reported by Eckert *et al.*, which contained a feature centered at *ca.* -95 ppm with a FWHM of *ca.* 200 ppm [21]. We also obtained the nonspinning spectrum of our sample;

it was centered at −104 ppm with a FWHM of 180 ppm. Thus, the MAS and nonspinning spectra were very similar indicating that the average chemical-shift anisotropy of the sites within the amorphous solid was significantly smaller than the distribution of isotropic shifts.

We next collected spin-echo-decay data on the nonspinning sample for comparison to the data of Eckert *et al.* [21]. When the sample is held stationary rather than spun, all spin interactions (chemical shift, ^{113}Cd–^{31}P, *etc.*) except ^{31}P–^{31}P dipole couplings are refocused by the 180° pulse of the spin-echo pulse sequence. Thus, the decay of the echo envelope is entirely due to the ^{31}P–^{31}P dipole interaction, which is a function of P–P distances and numbers of P neighbors in the sample [30]. Consequently, the nonspinning ^{31}P spin-echo decay measurements contain structural information about local P environments.

The experimental echo heights for the organometallic-derived amorphous $CdGeP_2$ fit a gaussian decay with $T_2 = 350$ μs as defined by $\exp[-(2\tau/T_2)^2]$ where τ is the pulse spacing. The data are plotted in Fig. 5. For comparison, the data reported by Eckert *et al.* for conventionally derived glassy $CdGeP_2$ are also plotted in Fig. 5 [21], and the two data sets agree within the limits of experimental error. The results strongly suggest that the conventionally derived and the organometallic-derived glassy $CdGeP_2$ materials have the same structure. Of course, different structures may exhibit the same spin-echo decays if, for example, fewer P neighbors were perfectly offset by shorter P–P distances in one structure relative to the other. However, we consider this scenario to be very unlikely in view of the other evidence: (1) the materials obtained from the two syntheses exhibit the same crystallization temperature; (2) they exhibit very similar average ^{31}P chemical shifts; and (3) they exhibit very similar

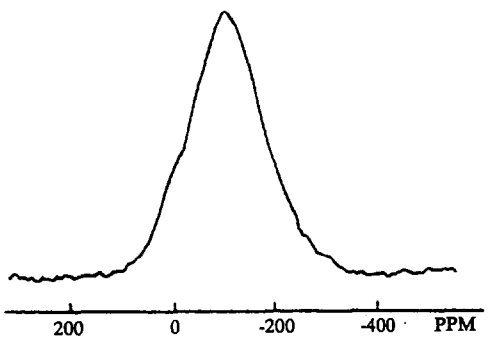

Fig. 4. Solid-state MAS ^{31}P NMR spectrum of organometallic-derived amorphous $CdGeP_2$ (spinning rate = 8 kHz). The peak is centered at −104 ppm and has a full width at half maximum of 160 ppm.

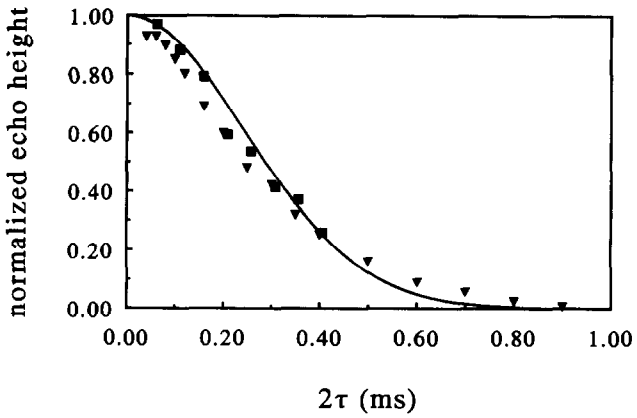

Fig. 5. ^{31}P spin-echo-decay data for organometallic-derived amorphous $CdGeP_2$ (■) and conventionally derived (melt-quenched) glassy $CdGeP_2$ of Eckert *et al.* from ref. 21 (▼). The curve is the gaussian fit to the points for the organometallic-derived $CdGeP_2$ ($T_2 = 350$ μs).

isotropic-shift distributions. We conclude that the glassy $CdGeP_2$ materials made from the high- and low-temperature techniques are either isostructural or very nearly so.

Eckert *et al.* examined their spin-echo data to analyze the statistics of P–P *versus* P–Cd and P–Ge bonds in glassy $CdGeP_2$ [21]. They used a combination of a random-site-occupancy model and the ideal crystalline chalcopyrite structure to model chemical disorder in the glass. The random-site-occupancy model retains the chalcopyrite atomic lattice but stipulates that the atomic sites are randomly occupied by the constituent elements. The best fit to their data was obtained with a 55:45 admixture of the two models, respectively. Thus, they inferred that significant quantities of P–P bonds were present in glassy $CdGeP_2$. However, our organometallic syntheses proceeded by formation of M–P covalent bonds exclusively; no organic byproducts (*e.g.*, $Me_3SiSiMe_3$) consistent with the formation of P–P covalent bonds were detected (see above). Consequently, substantial rearrangements to higher-energy local structures, requiring atomic migrations at ≤ 350°C, would be necessary to produce significant numbers of P–P bonds in our amorphous $CdGeP_2$, if such P–P bonds were actually to exist. We suspect that other structural models should be considered for glassy $CdGeP_2$, including models that are not based on chalcopyrite-like lattices, and therefore are not based on simple chemical disorder.

Our results show that, as in sol-gel routes to oxide glasses, II–IV–V_2 glasses can be made from the "bottom up". Studies on sol-gel-derived oxide glasses have shown that when they are manipulated at temperatures approaching the glass temperatures (T_g), they exhibit

very similar or identical structures to the analogous glasses quenched from high-temperature melts [22,31,32]. Our organometallic-derived glassy $CdGeP_2$ was prepared at 350°C; apparently that was close enough to T_g (*ca.* 450°C) to result in essentially the same structure as exhibited by the conventionally derived $CdGeP_2$ glass. One advantage of the organometallic synthesis is that only a few II–IV–V_2 compounds can be quenched rapidly enough to give glasses from high temperatures [20]; thus, the organometallic routes will provide glasses that cannot obtained by conventional techniques. In the present study, both $ZnGeP_2$ and $CdGeP_2$ were obtained as glasses well below their crystallization temperatures, whereas $ZnSnP_2$ and $CdSnP_2$ were beginning to crystallize at the temperatures required to complete the elimination of Me_3SiX. Because the known glassy II–IV–V_2 phases have different densities, band gaps, and optical properties than their crystalline chalcopyrite counterparts [20,21], new glassy II–IV–V_2 phases are worthy of study and our new techniques provide a means of preparing them.

3. Conclusion

We have described the first organometallic routes to ternary II–IV–V_2 semiconductors, which are analogous to the sol-gel process for oxides. The precursors $\{M^{II}[P(SiMe_3)_2]_2\}_2$ (M^{II} = Zn, Cd) and $M^{IV}X_4$ (M^{IV} = Ge, Sn; X = OMe, Cl) underwent smooth elimination reactions to afford sols, gels, solutions, or precipitates that were converted to amorphous $M^{II}M^{IV}P_2$ phases at 250–350°C. The amorphous materials were subsequently annealed to give crystalline chalcopyrite phases at the lowest temperatures yet reported for the compounds studied. Amorphous $CdGeP_2$ prepared by the organometallic synthesis was found to be isostructural with glassy $CdGeP_2$ prepared by conventional melt quenching, suggesting that other and new II–IV–V_2 glasses can be made by this technique. The organometallic reactions described herein form the basis for a new method of preparing ternary-semiconductor sols, gels, glasses, and polycrystalline powders.

4. Experimental details

All procedures were carried out under dry nitrogen using standard inert-atmosphere techniques. Compounds $\{Zn[P(SiMe_3)_2]_2\}_2$ and $\{Cd[P(SiMe_3)_2]_2\}_2$ were prepared as reported earlier [12,24]. $Ge(OMe)_4$ [33] and $Sn(OMe)_4$ [34] were prepared by literature procedures. $GeCl_4$ and $SnCl_4$ were purchased from Aldrich and used without further purification. Toluene, hexane, and THF were distilled from sodium benzophenone ketyl. After all annealing runs, the samples were cooled to room temperature in *ca.* 1 h.

C, H analyses were performed by Onieda Research Services, Whitesboro, NY. Zn and Cd were estimated by EDTA titration [35]. Efforts to estimate Cl gravimetrically as AfCl were unsuccessful because of interference by PH_3 generated in the digestion of the samples. X-Ray powder data (XRD) were collected on a Rigaku DMaxA diffractometer. Simulated XRD patterns for the II–IV–V_2 chalcopyrites were obtained by using the known atomic positional parameters [23] as input to the program XPOW, which is part of the SHELXTL PLUS program package (Siemens Analytical X-Ray Instruments, Inc.). Solid-state MAS ^{31}P NMR spectra were obtained in an 8.0 T field (137.9 MHz) with a locally built spectrometer and a Doty Scientific spinning assembly. The sample was placed in 5 mm zirconia rotors, and spectra were referenced to external 85% H_3PO_4.

4.1. Preparation of $ZnGeP_2$

4.1.1. Method A

$Ge(OMe)_4$ (550 μl, 0.73 g, 3.7 mmol) and $\{Zn[P(SiMe_3)_2]_2\}_2$ (1.57 g, 1.87 mmol) were combined in toluene (20 ml) at room temperature. The solution changed from colorless to red brown in *ca.* 1 day. The reaction mixture was then heated to reflux whereupon a brown precipitate formed. The solution was refluxed for 48 h and the very air-sensitive brown solid was collected by filtration, washed with 2 × 20 ml of benzene, and dried under vacuum (yield 0.70 g). Anal. Found: C, 11.01; H, 2.04; Zn, 25.47. $ZnGeP_2(SiMe_3)_{0.5}(OMe)_{0.5}$ calc.: C, 9.52; H, 2.38; Zn, 25.95%. IR (KBr): ν(SiMe) 1251m; ν(O–C) 1016m; ν(Si–C) 840s cm^{-1}.

A portion of the brown powder (0.31 g) was heated under a dynamic vacuum (10^{-2} Torr) at 350°C for 12 h to produce a dark brown solid (yield 0.25 g), which was amorphous according to XRD. Anal. Found: C, 3.29; H, 0.43; Zn, 31.86 $ZnGeP_2$ calc.: C, 0; H, 0; Zn, 32.70%. A ^1H NMR spectrum of the organics collected in a liquid-N_2 cold trap during heating showed only Me_3SiOMe and a trace of toluene. A portion of the material from the 350°C treatment (0.12 g) was heated to 800°C in an evacuated quartz tube for 18 h to give a black solid, which was crystalline $ZnGeP_2$ according to XRD (JCPDS#33-1471). Analysis showed 3.01% residual carbon. The stability of the solid to conc. HNO_3 and HCl precluded a Zn analysis. Energy-dispersive X-ray spectroscopy showed only background levels of Si.

4.1.2. Method B

$GeCl_4$ (500 μl, 0.94 g, 4.4 mmol) and $\{Zn[P(SiMe_3)_2]_2\}_2$ (1.82 g, 2.19 mmol) were combined in toluene (30 ml) at room temperature. The solution changed from colorless to brown in 1 h and a rigid gel formed. The gel was allowed to stand overnight (15 h) without any noticeable change. The reaction mixture was then heated to reflux for 24 h resulting in the formation of a very air-sensitive brown powder, which was collected by filtration and washed with 2 × 5 ml hexane and dried (yield 1.09 g). Anal. Found: C, 8.30; H, 2.02; Zn, 24.92. $ZnGeP_2(SiMe_3)_{0.6}Cl_{0.6}$ calc.: C, 8.15; H, 2.05; Zn, 24.67%. IR (KBr): ν(SiMe) 1250m; ν(Si–C) 841vs cm^{-1}.

A portion of the brown solid (0.52 g) was heated under a dynamic vacuum (10^{-2} Torr) for 12 h at 400°C to yield 0.40 g of dark brown solid. A ^1H NMR spectrum of the volatile organics collected in a liquid-N_2 cold trap during heating showed only Me_3SiCl. A portion of the heated material (0.25 g) was further heated in an evacuated quartz tube at 800°C for 15 h to yield 0.19 g of a black solid, which was crystalline $ZnGeP_2$ according to XRD. Analysis of the black solid showed 2.14% residual carbon. The stability of the solid to conc. HNO_3 and HCl precluded a Zn analysis.

4.2. Preparation of $CdGeP_2$

4.2.1. Method A

The procedure was similar to the preparation of $ZnGeP_2$ (Method A) and used $Ge(OMe)_4$ (290 μl, 0.39 g, 2.0 mmol), $\{Cd[P(SiMe_3)_2]_2\}_2$ (0.93 g, 1.0 mmol), and toluene (25 ml). A very air-sensitive black solid (0.48 g) was collected after 48 h of refluxing. Anal. Found: C, 5.94; H, 0.63; Cd, 40.79. $CdGeP_2(OMe)_{0.3}(SiMe_3)_{0.3}$ calc.: C, 5.18; H, 1.30; Cd, 40.40%. IR (KBr): ν(SiMe) 1243 m; ν(O–C) = 1019m; ν(Si–C) = 836s cm^{-1}.

A portion of black solid (0.30 g) was heated at 350°C for 12 h in an evacuated pyrex tube to yield 0.21 g of black solid, which was amorphous to XRD. Anal. Found: C, 1.47; H, 0.14; Cd, 44.40. $CdGeP_2$ calc.: C, 0; H, 0; Cd, 45.51%. The heated solid (0.20 g) was further heated at 600°C for 12 h in an evacuated quartz tube to yield 0.18 g of black solid, which was crystalline $CdGeP_2$ according to XRD (JCPDS#24-162). Analysis showed 0.93% of residual carbon. Sharper diffraction intensities were observed when the material was similarly heated to 650°C. The stability of the solid to conc. HNO_3 and HCl precluded a Cd analysis. Energy-dispersive X-ray spectroscopy showed only background levels of silicon.

4.2.2. Method B

$GeCl_4$ (0.56 g, 2.63 mmol) and $\{Cd[P(SiMe_3)_2]_2\}_2$ (1.23 g, 1.32 mmol) were combined in 50 ml of toluene at room temperature. A solid precipitated, which was initially white but became brown in 3–4 min. The reaction mixture was then refluxed for 15 h and the resulting air-sensitive dark-brown precipitate was collected by filtration, washed with 15 ml of hexane, and dried (yield 0.83 g). Anal. Found: C, 9.57, H, 2.03; Cd, 34.64. $CdGeP_2(SiMe_3)_{0.8}Cl_{0.8}$ calc.: C, 8.63; H, 2.17; Cd, 33.68%. IR (KBr): ν(SiMe) 1251m; ν(Si–C) 840s cm^{-1}.

A portion of the brown solid was heated under a dynamic vacuum (10^{-2} Torr) at 300°C for 4 h to yield 0.35 g of black powder. Anal. Found: Cd, 43.78. $CdGeP_2$ calc.: Cd, 45.51%. A 0.20 g portion was further heated in an evacuated quartz tube at 600°C for 15 h. The resulting black solid (0.18 g) was crystalline $CdGeP_2$ according to XRD, and contained 1.26% residual carbon.

4.3. Preparation of $ZnSnP_2$

4.3.1. Method A

The procedure was analogous to the preparation of $ZnGeP_2$ (Method A) and used $Sn(OMe)_4$ (0.58 g, 2.4 mmol), $\{Zn[P(SiMe_3)_2]_2\}_2$ (1.00 g, 1.19 mmol), and toluene (20 ml). The mixture was refluxed for 2 days resulting in an air-sensitive black precipitate, which was collected by filtration, washed with 10 ml of hexane, and dried (yield 0.62 g). Anal. Found: C, 8.55; H, 1.95; Zn, 21.8. $ZnSnP_2(SiMe_3)_{0.5}(OMe)_{0.5}$ calc.: C, 8.06; H, 2.02; Zn, 21.94%. IR (KBr): ν(SiMe) 1252m; ν(O–C) 1024m; ν(Si–C) 840vs cm^{-1}.

A portion of the black powder (0.3 g) was heated at 300°C under a dynamic vacuum (10^{-2} Torr) for 4 h and then at 450°C in an evacuated pyrex tube for 12 h. The resulting solid (0.22 g) showed a slightly broadened XRD pattern corresponding to $ZnSnP_2$ and a small amount of β-Sn (JCPDS#4-0673). The solid was further heated at 600°C in an evacuated quartz tube. The XRD pattern of the resulting solid was sharpened; the β-Sn impurity remained. The solid was similarly heated to higher temperatures; decomposition to unidentifiable phases resulted.

4.3.2. Method B

$SnCl_4$ (0.62 g, 2.4 mmol) and $\{Zn[P(SiMe_3)_2]_2\}_2$ (1.00 g, 1.19 mmol) were combined in toluene (50 ml) at room temperature giving an exothermic reaction. The solution changed from colorless to brown and became a very viscous sol (approaching a gel). The reaction mixture was kept at room temperature for 5 h without any noticeable change in color or viscosity. The reaction mixture was then heated to reflux for 24 h whereupon an air-sensitive black solid precipitated, which was collected by filtration, washed with 2 × 5 ml of

hexane, and dried (yield 0.71 g). Anal. Found: C, 8.38; H, 1.88; Zn, 20.39. $ZnSnP_2(SiMe_3)_{0.8}Cl_{0.8}$ calc.: C, 8.66; H, 2.18; Zn, 19.64%. IR (KBr): ν(SiMe) 1248m; ν(Si–C) 841vs cm^{-1}.

A portion of the black solid (0.36 g) was heated at 350°C under a dynamic vacuum (10^{-2} Torr) for 7 h to give 0.23 g of solid, which showed a broad XRD pattern for $ZnSnP_2$. This solid was further heated at 600°C in an evacuated quartz tube for 12 h. The resulting solid showed a sharp XRD pattern for $ZnSnP_2$ with a small amount of Sn_4P_3 (JCPDS#20-1294) as an impurity phase.

4.4. Preparation of $CdSnP_2$

4.4.1. Method A

The procedure was analogous to the preparation of $ZnGeP_2$ (Method A) and used $Sn(OMe)_4$ (0.44 g, 1.8 mmol), $\{Cd[P(SiMe_3)_2]_2\}_2$ (0.84 g, 0.90 mmol), and toluene (25 ml). The reaction mixture was refluxed for 24 h and the resulting air-sensitive black precipitate was collected by filtration, washed with 10 ml of hexane, and dried (yield 0.60 g). Anal. Found: C, 5.59; H, 1.09; Cd, 33.31. $CdSnP_2(SiMe_3)_{0.4}(OMe)_{0.4}$ calc.: C, 5.74; H, 1.45: Cd, 33.38%. IR (KBr): ν(SiMe) 1259m; ν(O–C) 1095m, 1028m; ν(Si–C) 837vs cm^{-1}.

A portion of black solid (0.40 g) was heated at 300°C under a dynamic vacuum (10^{-2} Torr) for 4 h. The XRD pattern of the resulting solid (0.32) was broad and corresponded to $CdSnP_2$ (JCPDS#22-517) along with a small amount of Sn_4P_3 (JCPDS#20-1294) as an impurity. When the black solid was further heated to 450°C in an evacuated pyrex tube, the XRD pattern sharpened; however, the Sn_4P_3 impurity remained.

4.4.2. Method B

$SnCl_4$ (0.56 g, 2.1 mmol) and $\{Cd[P(SiMe_3)_2]_2\}_2$ (1.00 g, 1.07 mmol) were combined in toluene (50 ml) at 0°C. The solution turned from pale yellow to brown immediately and a brown precipitate formed. The reaction mixture was then refluxed for 8 h and the resulting air-sensitive black solid was collected by filtration, washed with 2×10 ml of hexane, and dried (yield 0.75 g). Anal. Found: C, 5.57; H, 1.21; Cd, 34.68. $CdSnP_2(SiMe_3)_{0.5}Cl_{0.5}$ calc.: C, 5.19; H, 1.30; Cd, 34.17%. IR (KBr): ν(SiMe) 1257m; ν(Si–C) 839vs cm^{-1}.

A portion of the black solid (0.48 g) was heated at 250°C under a dynamic vacuum (10^{-2} Torr) for 2 h to give 0.38 g of solid, which exhibited a broad XRD pattern corresponding to $CdSnP_2$. The solid was then heated to 450°C in an evacuated pyrex tube. The XRD pattern for $CdSnP_2$ sharpenend and an appreciable amount of Sn_4P_3 impurity was evident. No effort was made to quantify the amount of Sn_4P_3 present.

4.5. ^{31}P NMR spin-echo decay for $CdGeP_2$

A sample of $CdGeP_2$ prepared by Method A and heated at 350°C was used. Spin echoes were generated on the nonspinning sample by the following pulse sequence: $90°-\tau-180°-\tau-$echo. Data (2τ in ms, normalized echo height): 0.062, 0.970; 0.110, 0.882; 0.160, 0.792; 0.210, 0.594; 0.258, 0.536; 0.308, 0.414; 0.356, 0.372; 0.406, 0.259. The data are plotted in Fig. 5.

Acknowledgments

Support to W.E.B. was provided by the donors of the Petroleum Research Fund, administered by the American Chemical Society, and an NSF Presidential Young Investigator award supported by the Monsanto Co. and the Eastman Kodak Co. Support to M.S.C. was provided by NSF DMR-9024502. The Washington University High-Resolution NMR Service Facility was funded in part by NIH Biomedical Research-Support Shared-Instrument Grant 1 S10 RR02004 and a gift from the Monsanto Co. Washington University provided equipment support. W.E.B. thanks Professor James K. Bashkin, Washington University, for helpful suggestions.

References

1 J. L. Shay and J. H. Wernick, *Ternary Chalcopyrite Semiconductors: Growth, Electronic Properties, and Applications*, Pergamon, Oxford, 1975, Ch. 1.
2 J. Covino, *Proc. SPIE Int. Soc. Opt. Eng., 505* (1984) 35.
3 G.C. Bhar, S. Das, U. Chatterjee and K. L. Vodopyanov, *Appl. Phys. Lett., 54* (1989) 313.
4 M. A. Ryan, M. W. Peterson, D. L. Williamson, J. S. Frey, G. E. Maciel and B. A. Parkinson, *J. Mater. Res., 2* (1987) 528.
5 H. -S. Shen, G. -Q. Yao, R. Kershaw, K. Dwight and A. Wold, *J. Solid State Chem., 71* (1987) 176.
6 E. K. Byrne, L. Parkanyi and K. H. Theopold, *Science, 241* (1988) 332.
7 R. L. Wells, C. G. Pitt, A. T. McPhail, A. P. Purdy, S. Shafieezad and R. B. Hallock, *Chem. Mater., 1* (1989) 4.
8 A. H. Cowley and R. A. Jones, *Angew. Chem., Int. Ed. Engl., 28* (1989) 1208.
9 M. D. Healy, P. E. Laibinis, P. D. Stupik and A. R. Barron, *J. Chem. Soc., Chem. Commun.*, (1989) 359.
10 S. M. Stuczynski, J. G. Brennan and M. L. Steigerwald, *Inorg. Chem., 28* (1989) 4431.
11 M. A. Olshavsky, A. N. Goldstein and A. P. Alivisatos, *J. Am. Chem. Soc., 112* (1990) 9438.
12 S. C. Goel, M. Y. Chiang and W. E. Buhro, *J. Am. Chem. Soc., 112* (1990) 5636.
13 S. M. Stuczynski, R. L. Opila, P. Marsh, J. G. Brennan and M. L. Steigerwald, *Chem. Mater., 3* (1991) 379.
14 R. D. Dupuis, *Science, 226* (1984) 623.
15 M. G. Bawendi, A. R. Kortan, M. L. Steigerwald and L. E. Brus, *J. Chem. Phys., 91* (1989) 7282.

16 J. G. Brennan, T. Siegrist, P. J. Carroll, S. M. Stuczynski, P. Reynders, L. E. Brus and M. L. Steigerwald, *Chem. Mater., 2* (1990) 403.
17 H. Uchida, C. J. Curtis, P. V. Kamat, K. M. Jones and A. J. Nozik, *J. Phys. Chem., 96* (1992) 1156.
18 M. A. Matchett, A. M. Viano, N. L. Adolphi, R. D. Stoddard, W. E. Buhro, M. S. Conradi and P. C. Gibbons, *Chem. Mater., 4* (1992) 508.
19 C. J. Brinker and G. W. Scherer, *Sol-Gel Science*, Academic Press, Boston, 1990, Ch. 14.
20 J. L. Shay and J. H. Wernick, *Ternary Chalcopyrite Semiconductors: Growth, Electronic Properties, and Applications*, Pergamon, Oxford, 1975, pp. 71–72.
21 D. Franke, R. Maxwell, D. Lathrop and H. Eckert, *J. Am. Chem. Soc., 113* (1991) 4822.
22 C. J. Brinker and G. W. Scherer, *Sol-Gel Science*, Academic Press, Boston, 1990, Ch. 12.
23 J. L. Shay and J. H. Wernick, *Ternary Chalocopyrite Semiconductors: Growth, Electronic Properties, and Applications*, Pergamon, Oxford, 1975, pp. 3–10.
24 S. C. Goel, M. Y. Chiang, D. J. Rauscher and W. E. Buhro, *J. Am. Chem. Soc.*, 115 (1993) 160.
25 R. Roy, *Science, 238* (1987) 1664.
26 L. G. Hubert-Pfalzgraf, *New J. Chem., 11* (1987) 663.
27 D. C. Bradley, *Chem. Rev., 89* (1989) 1317.
28 J. L. Shay and J. H. Wernick, *Ternary Chalcopyrite Semiconductors: Growth, Electronic Properties, and Applications*, Pergamon, Oxford, 1975, pp. 60–64.
29 N. A. Goryunova, S. M. Ryvkin, G. P. Shpenikov, I. I. Tichina and V. G. Fedotov, *Phys. Status Solidi, 28* (1968) 489.
30 C. P. Slichter, *Principles of Magnetic Resonance*, Springer, New York, 1980.
31 A. R. Cooper, *Mater. Res. Soc. Symp. Proc., 73* (1986) 421.
32 M. C. Weinberg, *Mater. Res. Soc. Symp. Proc., 73* (1986) 431.
33 D. C. Bradley, L. Kay and W. Wardlaw, *Chem. Ind.*, (1953) 746.
34 D. C. Bradley, E. V. Caldwell and W. Wardlaw, *J. Chem. Soc.*, (1957) 4775.
35 J. Basset, R. C. Denney, G. H. Jeffery and J. Mendham, *Vogel's Textbook of Quantitative Inorganic Analysis*, 4th edition, Wiley, New York, 1978, pp. 324–325.
36 A. A. Vaipolin, N. A. Goryunova, L. I. Kleshchinskii, G. V. Loshakova and E. O. Osmanov, *Phys. Status Solidi, 29* (1968) 435.
37 E. Buehler, J. H. Wernick and J. L. Shay, *Mater. Res. Bull., 6* (1971) 303.
38 S. Shirakata and S. Isomura, *J. Cryst. Growth, 99* (1990) 781.